Perturbing the Movement of Hydrogens to Delineate and Assign Events in the Reductive Activation and Turnover of Porcine Dihydropyrimidine Dehydrogenase.

*Brett A. Beaupre, Dariush C. Forouzesh, Arseniy Butrin, Dali Liu, and Graham R. Moran**

Department of Chemistry and Biochemistry, 1068 W Sheridan Rd, Loyola University Chicago, Chicago, IL 60660

*corresponding author; phone: (773)508-3756; email: gmoran3@luc.edu

Abstract

The native function of dihydropyrimidine dehydrogenase (DPD) is to reduce the 5,6 vinylic bond of pyrimidines uracil and thymine with electrons obtained from NADPH. NADPH and pyrimidines bind at separate active sites separated by around 60 Å that are bridged by four Fe_4S_4 centers. We have shown that DPD undergoes reductive activation, taking up two electrons from NADPH (Beaupre et al., 2020 Biochemistry, 59 pp 2419-2431). pH Studies indicate that the rate of turnover is not controlled by the protonation state of the general acid, cysteine 671. The activation of the C671 variants delineates into two phases particularly at low pH values. Spectral deconvolution of the delineated reductive activation reaction reveals that the initial phase results in the accumulation of charge transfer absorption added to the binding difference spectrum for NADPH. The second phase results in reduction of one of the two flavins. X-ray crystal structural analysis of the C671S variant soaked with NADPH and the slow substrate, thymine in low oxygen atmosphere resolved the presumed activated form of the enzyme that has the FMN cofactor reduced. These data reveal that charge transfer arises from close proximity of the NADPH and FAD bases and that the ensuing flavin is a result of rapid transfer of electrons to the FMN without accumulation of reduced forms of the FAD or Fe_4S_4 centers. These data suggest that the slow rate of turnover of DPD is governed by the movement of a mobile structural feature that carries the C671 residue.

Introduction

Dihydropyrimidine dehydrogenase (DPD) catalyzes the reduction of the 5,6-vinylic bond of the pyrimidines, thymine and uracil with electrons derived from NADPH [1-3] (Scheme 1).

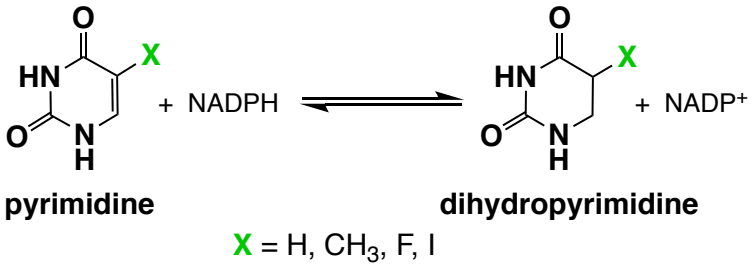

Scheme 1: The Chemistry Catalyzed by DPD

DPD has considerable medical relevance as it rapidly detoxifies ($t_{1/2}$ ~20 min) the antineoplastic agent, 5-fluorouracil (5FU) [4-11]. Net DPD activity varies between individuals (30-fold)[8, 12] and is therefore both a therapeutic complication in dosing and a primary determinant of 5FU toxicity/efficacy [4, 5, 9, 13-16]. Inhibition of DPD has long been recognized as a means to improve outcomes of chemotherapeutic regiments for numerous cancers[14, 15]. The chemistry catalyzed by DPD is typical of numerous flavin-dependent dehydrogenases[17-20] but its architecture is atypical. DPD exists as a homo-dimer of 113 kDa protomers that each contain six redox cofactors; an FAD, an FMN and four Fe_4S_4 clusters (Figure 1). The DPD dimer interlocks with a head to head orientation, positioning the four Fe_4S_4 clusters (two provided from each protomer) to form an apparent electron conduit, linking the FAD and FMN that are separated by 56 Å [21, 22]. Crystal structures of DPD-ligand complexes have revealed that NADPH binds adjacent to the FAD cofactor and that the pyrimidine substrates associate within the cavity containing FMN. Additionally, the FMN active site general acid C671 is observed to be proximal to the bound pyrimidine to facilitate proton-coupled electron transfer from NADPH [21].

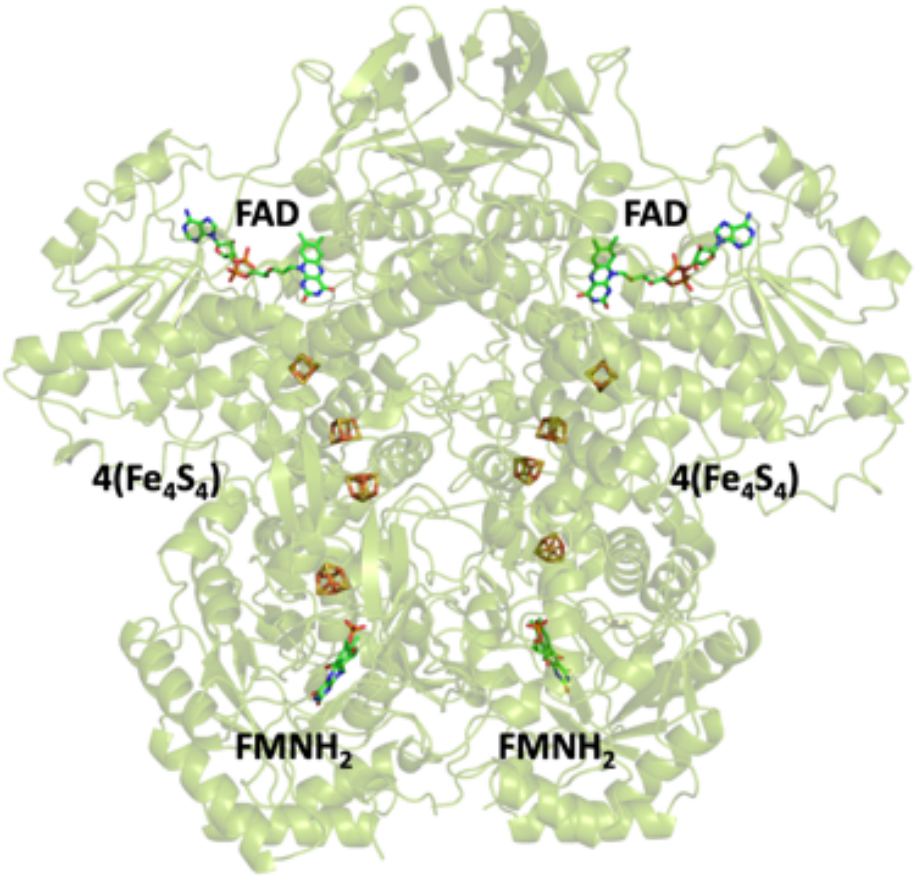

Figure 1. The Structure of Porcine Dihydropyrimidine Dehydrogenase.

For nearly three decades DPD has largely defied attempts to describe its behavior. Early reports on the kinetic mechanism of DPD used almost exclusively aerobic steady-state methods and failed to capture primary mechanistic details [1-3, 23-27]. Similarly, initial transient state data collected under anaerobic conditions concluded that the presence of uracil stimulated the rate of the electron transfer from NADPH by two orders of magnitude but did not reconcile these observations with any discrete mechanistic conclusions [27]. The limited scope of conclusions drawn in prior DPD investigations was in part a result of a paucity of pure active enzyme either from native or heterologous sources [1, 24, 26, 28]. Recent improvements in the recombinant production of DPD have to some extent overcome yield barriers and allowed for more detailed

reassessment of the mechanism [29]. Single turnover reactions have revealed biphasic first-order kinetics [30]. The delineation of the two phases was markedly enhanced in the C671S variant that significantly slows the rate of reduction of the pyrimidine. These data indicate that the initial phase is two electron activation that likely results in the reduction of the FMN cofactor. It was concluded that the proposed activated form of DPD (FAD, $4(Fe_4S_4)^{2+}$, $FMNH_2$) has high affinity for NADPH and so sequesters the co-substrate to bring about turnover as the second phase observed. The overall stoichiometry of these two processes was confirmed by acid-quench and HPLC product analysis. Furthermore, it was shown that the activated form of DPD persists when NADPH is exhausted in the presence of saturating oxidant pyrimidine substrate. This indicates that the electrons acquired for activation are retained and are not available to reduce pyrimidine substrates. On this basis, it was established that catalysis is preceded by a reductive activation step [30].

The data presented in this study further supports a kinetic model for DPD turnover that requires an initial NADPH dependent reduction step that occurs most efficiently in the presence of substrate pyrimidines. Using variant forms of DPD that slow or halt the turnover reaction of the enzyme, structures of the presumed activated form of the enzyme were obtained. These structures capture the proposed activated form where the FMN is two-electron reduced. Additionally, we investigate deuterium solvent and kinetic isotope effects on the activation and turnover reactions. Combined with prior observations, the data support a mechanism in which DPD behaves as a Newton's cradle for electrons where incoming reducing equivalents from NADPH rapidly displace electrons onto the pyrimidine substrate but at rate that is governed by

movement of the loop that carries the active site general acid C671 required for proton coupled electron transfer.

Materials and Methods

Materials, quantitation and reaction conditions: Competent BL21 (DE3) cells were obtained from New England Biolabs. Tris(hydroxymethyl)aminomethane (Tris) buffer, dipotassium hydrogen phosphate (KPi), ethylenediaminetetraacetic acid (EDTA), nicotinamide adenine dinucleotide phosphate ($NADP^+$), ammonium sulfate, 2-[4-(2-hydroxyethyl)piperazin-1-yl]ethanesulfonic acid (HEPES) buffer, 2-(N-morpholino)ethanesulfonic acid (MES) buffer, 1D-glucose, acetic acid, and the Miller formulation of lysogeny broth (LB) powder were purchased from Fisher Scientific. Dithiothreitol (DTT) and reduced nicotinamide adenine dinucleotide phosphate (NADPH) were purchased from RPI Research Products. The sodium salt of ampicillin and dextrose powder were obtained from Spectrum Chemical. Uracil, ATP, and glucose oxidase were acquired from Sigma-Millipore. Glucose-6-phosphate dehydrogenase (G6PD) and hexokinase were from Alfa Aesar. Deuterium oxide and deuterium chloride were from Acros Organics.

All concentrations of DPD substrates and products were determined spectrophotometrically using known extinction coefficients (NADPH; ε_{340} = 6,220 $M^{-1}cm^{-1}$, $NADP^+$; ε_{260} = 17,800 $M^{-1}cm^{-1}$, uracil; ε_{260} = 8,200 $M^{-1}cm^{-1}$, thymine; ε_{264} = 7,860 $M^{-1}cm^{-1}$). The extinction coefficient used to quantify DPD was ε_{426} = 75,000 $M^{-1}cm^{-1}$ [29]. All concentrations indicated in this text are post-mixing.

***Preparation of DPD and Experimental Protocols*:** Recombinant DPDs were expressed and purified and stored as described previously [29]. Prior to experiments DPD was thawed and diluted or exchanged into the required buffer. Exchanges were carried out using repeated steps of

centrifugal concentration using 10 kDa nominal molecular weight cut-off filters (Amicon) and subsequent dilution to the target concentration. All preparative steps were performed at 4 °C.

To ensure a constant osmotic pressure for experiments that required a range of pH values, a mixture of 50 mM MES, 50 mM acetic acid, 100 mM Tris, 2 mM DTT (MAT buffer) was used to buffer for pHs 5.2 - 8.5 [31]. Deuterium oxide buffers and substrate solutions were prepared by dissolving reagents in D_2O and adjusting to the target pH with concentrated DCl with correction for the response of the pH electrode in D_2O solvent[32].

Enzyme samples were made anaerobic in glass tonometers using a modified Schlenk line and alternating cycles of vacuum and pure argon according to published protocols[33]. The samples were further protected from residual and infiltrating dioxygen contamination by the inclusion of 1 mM glucose and the addition of 1 U/mL glucose oxidase that was added from a side arm once the exchange cycles were completed. The tonometer was then mounted onto a HiTech stopped-flow spectrophotometer (TgK Scientific). Solutions that included substrates and products were made anaerobic in buffer containing 1 mM glucose by sparging for 5 minutes with argon prior to the addition of 1 U/mL glucose oxidase and mounting onto the stopped-flow spectrophotometer.

***Steady-state observations of DPD catalysis*:** The influence of pH, viscosity and solvent derived deuterium on the turnover of DPD were each assessed in the steady state. Previous studies had indicated that reduction of the pyrimidine is fully rate limiting in turnover[30]. Turnover number (TN) is defined as the rate measured in the presence of saturating substrates standardized to the enzyme subunit concentration and is taken to be synonymous with the term, k_{cat}. The influence of hydrogen ions on the TN of the wild type and the C671S variant of DPD was assessed using

stopped-flow, pH-jump methods. A tonometer containing 1 µM DPD (WT or C671S) was prepared anaerobically in buffer containing 5 mM potassium phosphate, 2 mM DTT and 1 mM glucose, pH 7.5. Substrate solutions contained 100 µM NADPH and 100 µM uracil and were prepared in MAT buffer adjusted to the target pH using acetic acid and then sparged with argon prior to mounting onto the instrument. Reactions were monitored for 50 seconds at 340 nm and 20 °C, and the rate was assessed from the slope of the trace from 2-20 seconds. The influence of pH on the TN could be described by a single ionization expression (Equation 1)[34]. The K_a values determined from titratable phenomena X, (in this case apparent TN, TN_{app}) were determined by plotting the pH against TN_{app}; where X_{AH} and X_{A^-} represent the respective fully protonated and unprotonated arms of the titration.

Equation 1

$$X = \frac{(X_{AH}[H^+] + K_a X_{A-})}{[H^+] + K_a}$$

The influence of solvent derived deuterium atoms was evaluated under anaerobic conditions in the steady-state. The time required for deuterium exchange equilibrium was evaluated by monitoring the consumption of NADPH ($\Delta\varepsilon$=6220 $M^{-1}cm^{-1}$) at 340 nm for varied incubation times (0, 60, 100, 120, 180, 210 sec). Wild type DPD (570 nM) in MAT buffer containing 1 mM glucose was prepared in either H_2O or D_2O at pH 8.5 or pD 8.09 respectively. Tonometers were made anaerobic as described and mounted onto the stopped-flow spectrophotometer. Reactions were initiated by mixing with 150 µM NADPH and 150 µM uracil and monitored for 40 seconds. The linear portion (1 - 10 sec) of the data traces was fit to a straight line to determine the rate.

To account for viscosity changes resulting from the introduction of D_2O (η_{rel} = 1.25), the effect of solvent viscosity on the TN of DPD was assessed for viscosities 1-1.75 using added glycerol[35]. DPD C671S (4 µM) was prepared as above in 1/20 MAT buffer, 1 mM glucose, pH 7.5. Glycerol (0-31.8% v/v) was dissolved in 2/1 MAT buffer, 1 mM glucose, 150 µM NADPH, 150 µM uracil, pH 8.5 and sparged with argon for 5 mins and glucose oxidase 1 U/mL was then added prior to mounting to the stopped flow instrument. DPD activity was observed at 340 nm for 50 seconds and the rate of turnover was assessed by fitting a straight line to the data for 2-20 seconds. These data were then plotted against relative viscosity (η_{rel}) and fit to a straight line.

The number of protons in flight during turnover of DPD with uracil under anaerobic conditions was estimated using the proton inventory method [36]. The influence of the deuterium fraction of the solvent was assessed by reacting DPD with uracil in the presence of varied fraction of solvent deuterium. The fraction of solvent deuterium was controlled by preparing MAT buffer containing 1 mM glucose in both H_2O and D_2O and adjusted to corresponding pL values. These were then combined to obtain a specific deuterium fraction ratio (0, 10, 25, 50, 70, 90 and 100%) and added to 5 mL glass syringes. Substrate solutions were made anaerobic by sparging with argon for 5 minutes prior to the addition of 150 µM of both uracil and NADPH. Glucose oxidase (1 U/mL) was added prior to mounting onto a stopped-flow spectrophotometer. Anaerobic enzyme solutions were prepared by sparging the buffer of desired deuterium fraction for 5 minutes. After sparging 10 µL of concentrated DPD was added to obtain a final concentration of 1 µM prior to the addition of 1 U/mL of glucose oxidase. The syringe was then mounted onto the stopped-flow spectrophotometer. Reactions were monitored at 340 nm for 50 sec at 20 °C. The linear portion of the trace (5 - 10 sec) was fit to a straight line and the rate determined. The ratio

of rate constants (k_n/k_0), where 0 represents 100% H_2O and n is the fraction of D_2O, was plotted against the deuterium fraction, n of the buffer. To evaluate the inventory for the number of protons in flight, data were fit to variations of the Kresge-Gross-Butler equation, Equation 2, 3, 4 respectively[37, 38]. Equation 2 describes a medium effect whereby greater than two protons contribute to the observed effect. In Equation 3 describes the case for one (v = 1) or two-proton (v = 2) in flight in the transition state when reactant fractionation factors approximate unity. In this equation, the inverse of the transition state fractionation factor, $1/\varphi^T$, is equal to the kinetic isotope effect when there is a single proton contributing to the effect, or v = 1. The fit for this equation had the ordinate intercept, i, as a variable. Equation 4 accounts for fractionation factors less than one that contribute to the effect from the reactant and transition state. The fit to this equation provides φ^R/φ^T; the value of solvent kinetic isotope effect.

Equation 2 $$k_n/k_0 = (\frac{k_H}{k_D})^{-n}$$

Equation 3 $$k_n/k_0 = (i - n + n\varphi^T)^v$$

Equation 4 $$k_n/k_0 = (1 - n + n\varphi^T)/(1 - n + n\varphi^R)$$

Transient-state Observations: The pH dependence of the DPD C671S reductive activation reaction was assessed under transient state conditions. C671S variant DPD (10 µM) was prepared in 5 mM potassium phosphate, 2 mM DTT and 1 mM glucose, pH 7.5. This DPD solution was then made anaerobic in a tonometer as described above and mounted onto the stopped-flow

spectrophotometer. Substrate solutions of NADPH (50 µM final) and thymine (100 µM final) were prepared 2/1 MAT buffer titrated with HCl to the desired pH, placed in glass syringes and sparged with argon for 5 minutes before the addition of 1 U/mL glucose oxidase. The substrate and DPD solutions were mixed and monitored for 50 seconds at 340 nm and 20 °C to observe only the reductive activation reaction. Data were fit to a linear combination of two exponentials and a linear component that accounted for the facile breakdown of NADPH at lower pH values (Equation 5). From this equation, the absorbance amplitudes (A_n) and associated rate constants (k_n) were determined. The term *m* is the slope of the rate accounting for NADPH degradation at low pHs and C is the final absorbance at 340 nm for the exponential phases. The effect of pH on rate constants or absorption changes was described by a single ionization expression (Equation 1). The K_a values were determined from the titratable phenomena, X (in this case k_{2obs}).

Equation 5 $$A_{340nm} = A_1(e^{-k_1 t}) + A_2(e^{-k_2 t}) + mt + C$$

The pH dependence of the activation of DPD C671S indicated that increased kinetic resolution for the reductive activation of the enzyme was observed at lower pH values. Similarly, the activation reaction of the C671A variant was similarly delineated in this way but at pH 7.5. To ascertain what processes were contributing in each of the phases observed for activation, transient state reactions were conducted for each variant that captured the net spectrophotometric changes that occur during reductive activation only. DPD C671S (14 µM) was prepared anaerobically in 1/20 MAT buffer, 1 mM glucose, pH 7.5, in a tonometer as described above and mixed with NADPH (50 µM) and thymine (100 µM) in 2/1 MAT buffer, 1 mM glucose

pH 5.75 that was made anaerobic by sparging as described above. In this case thymine is a slow substrate inducing a TN of 0.00024 s^{-1} such that the reductive activation reaction can be observed largely separate from ensuing turnover events. DPD C671A (15 µM) was prepared anaerobically in MAT buffer, 1 mM glucose, pH 7.5, in a tonometer as described above and mixed with NADPH (13 µM) and thymine (100 µM) in MAT buffer, 1 mM glucose pH 7.5 that was made anaerobic by sparging as described above.

For each variant, absorption changes were observed at 340 and 590 nm using photomultiplier detection and at all wavelengths spanning 300-850 nm using charged coupled device (CCD) detection. The single wavelength data were fit to a linear combination of two exponentials according to Equation 6. In this equation the absorbance changes at X wavelength were fit to obtain amplitudes (A_n) and associated rate constants (k_n).

Equation 6 $$A_{Xnm} = A_1(e^{-k_1 t}) + A_2(e^{-k_2 t}) + C$$

The CCD data were collected for two time-frames for each variant (C671S; 0-2.5 & 0-25 seconds, C671A 0-2.5 & 0-12.5 seconds) and spliced together at 2.5 seconds to form datasets that had time resolution sufficient for processes with substantially different rate constants. The datasets were fit to a two-step irreversible model using the Spectrafit singular value decomposition routine available in KinTek Explorer software (KinTek Corp.). The spectra returned were then subtracted to reveal the net absorption changes in each phase.

Transient-state kinetic isotope effects for DPD C671S were determined by comparing single turnover reactions in the presence of NADPH or Pro-S NADPD. The C671S variant of DPD

was used in these experiments as this form has delineated the activation and turnover processes[30]. DPD C671S was prepared anaerobically in MAT buffer pH 7.5 as described above and mounted to the stopped-flow spectrophotometer. Kinetic isotope effects were assessed by monitoring the reaction of DPD C671S (15 μM) at 340 nm in the presence of uracil (100 μM) and NADPH/D (9 μM) under anaerobic conditions at 20 °C. NADPH and Pro-S NADPD were prepared enzymatically immediately prior to experimentation. In each case a solution of 200 μM $NADP^+$, 200 μM ATP, 10 mM Mg^{2+} and 1 mM of either glucose or 1D-glucose was prepared for the production of NADPH and NADPD respectively. This was then mixed with 1 U of glucose-6-phosphate dehydrogenase and 1 U of hexokinase in MAT buffer pH 7.5. Reaction progress was monitored at 340 nm until complete (~ 200 sec) at which time the enzymes were removed by centrifugation using 10 kDa nominal molecular weight cutoff filters. The concentration of NADPH and NADPD were determined by absorption and diluted with MAT buffer to the desired reaction concentration.

***The crystal structure of the activated C671S and C671A variants*:** Diffraction quality crystals of DPD variants, C671S and C671A with elongated morphology were obtained by the hanging-drop vapor diffusion method. Crystallization conditions were adopted from Dobritzsch et al., 2001 [22]; ~4.5 mg/mL (~40 μM) of DPD variants, C671S or C671A in 25 mM HEPES, 2 mM DTT, 10% glycerol at pH 7.5 were prepared and mixed 1:1 with well solution containing 100 mM sodium citrate, 2 mM DTT, 15% PEG 6000 at pH 4.5 to 4.9 to give a 6 μL drop. Crystallization was carried out in the dark to eliminate photo-degradation of the quasi-labile FMN cofactor[39]. Crystals appeared after 16 hours as both single elongated rectangular hexahedron forms (200 x 50 x 50 μM) or urchin-

like clusters. Only crystals from the single crystal form were harvested and placed in a Plas-Labs 830 series glove box in which a Motic binocular microscope coupled to an Accuscope 1080p high definition camera was placed. Before being placed in the glove box, the well solutions of the selected crystals were made anaerobic with the addition of 10 mM dithionite and resealed with the cover slide. The glove box was then made anaerobic by flushing with pure nitrogen gas for approximately 10 minutes at which time the fractional dioxygen was 0.1 %, as indicated by a Forensics Detectors oxygen meter. Atmospheric dioxygen was measured throughout the soaking procedure and was held below 1%. C671A and C671S DPD crystals were soaked for a minimum of 20 minutes in 25 mM HEPES, 100 mM sodium citrate, 2 mM DTT, 100 µM NADPH, 100 µM uracil (C671A) or thymine (C671S), 20% PEG 6000, 20% PEG 400, pH 7.5 prior to submersion in liquid nitrogen. Frozen crystals were then removed from the anaerobic environment and stored in liquid nitrogen.

Diffraction data were collected at 100 K at the beamline 21-ID-D of the Advanced Photon Source at Argonne National Laboratory. The beamline was equipped with a Dectris Eiger 9M detector. Data were collected using an oscillation angle of 0.5° over a range of 240° and an exposure time of 1 second per frame. The wavelength was fixed at 1.127 Å. Diffraction images were processed using xia2. Data processing statistics are given in Table 1. Phasing was conducted via molecular replacement using the program phaser. A model of Porcine DPD (PDB ID 1H7W) was used as a starting search model. The model building and refinement was undertaken in Coot [41] and Phenix [42] respectively in a repeated manner until the lowest R_{free} was achieved. The coordinates and structure factors have been deposited in the Protein Data Bank with accession

codes 7M32 and 7M31 (Table 1). Structural analysis and figures are made using PyMOL Version 2.0 (Schrödinger, LLC.).

Table 1. Crystallographic data collection and model refinement statistics for the DPD variant complexes

Complex	**DPD C671A**	**DPD C671S**
PDB code	7M32	7M31
Space group	P 1 2_1 1	P 1 2_1 1
Unit Cell dimension		
α, β, γ (deg)	90.0, 95.9, 90.0	90.0, 95.7, 90.0
a, b, c (Å)	81.9, 158.7, 162.7	82.0, 159.6, 162.9
Processed Resolution (Å)	1.82	1.69
R_{merge} [a] (%)	14.7 (194.6)	19.0 (185.1)
R_{pim} [c] (%)	7.4 (96.9)	9.6 (94.4)
I/σ (I)	7.4 (0.9)	6.0 (0.9)
CC ½ [d] (%)	99.6 (34.1)	99.2 (35.0)
Completeness (%)	96.5(96.2)	99.0 (99.8)
Multiplicity	4.8 (4.9)	4.7 (4.8)
No. Reflections	1705022	2169918
No. Unique Reflections	354924	459508
Refinement		
R_{work} [e]/R_{free} [f] (%)	16.81/20.09	17.65/19.99
No. of Atoms		
protein	30714	30857
ligand	496	684
water	2630	4306
Average B factors (Å^2)		
protein	34.39	25.74
RMSD [g]		
bond lengths (Å)	0.006	0.005
bond angles (deg)	1.00	1.02
Ramachandran plot (%)		
favored	96.33	96.15
allowed	3.35	3.50
outliers	0.32	0.35

[a]$R_{merge} = \Sigma|I_{obs} - I_{avg}|/\Sigma I_{avg}$, [b]The values for the highest-resolution bin are in parentheses, [c]Precision-indicating merging R, [d]Pearson correlation coefficient of two "half" data sets, [e]$R_{work} = \Sigma|F_{obs} - F_{calc}|/\Sigma F_{obs}$, [f]Five percent of the reflection data were selected at random as a test set, and only these data were used to calculate R_{free}, [g]Root-mean square deviation.

Results

Recently we have shown that DPD undergoes reductive activation whereby the initial two electrons to enter the protein from NADPH reside on one of the two flavin cofactors and it is this form of the enzyme that is competent in catalysis [30]. Our earlier data suggested that these electrons enter at the FAD site but reside on the FMN. In this article we explore rate limiting processes in both the activation and turnover of DPD and present structural evidence for the activated state of the enzyme. These data suggest that the rates of activation and turnover are respectively influenced by the protonation state of groups that are near or part of the FAD and the FMN cofactors.

***Steady-state rate dependence on pH and solvent deuterium fraction*:** Available crystal structures and observation of variant forms of DPD indicate that C671 is the active site general acid that delivers a proton to the pyrimidine substrate concomitant with hydride transfer from the reduced FMN cofactor[21, 22, 30, 40]. If the pKa of C671 controlled the rate of catalysis it would be reasonable to conclude that a pH profile for the TN would show a maximum rate at lower pH values. Figure 2A depicts the pH dependence of the apparent TN of DPD WT and C671S variant as a function of pH. MAT buffer was chosen as a suitable buffer system as it maintains a constant osmotic pressure across all pH values used[31]. These data indicate that the apparent TN increases ~fourfold from low to high pH values for both the WT and C671S variants. Similar observations were made by Podschun et al. 1993[2].

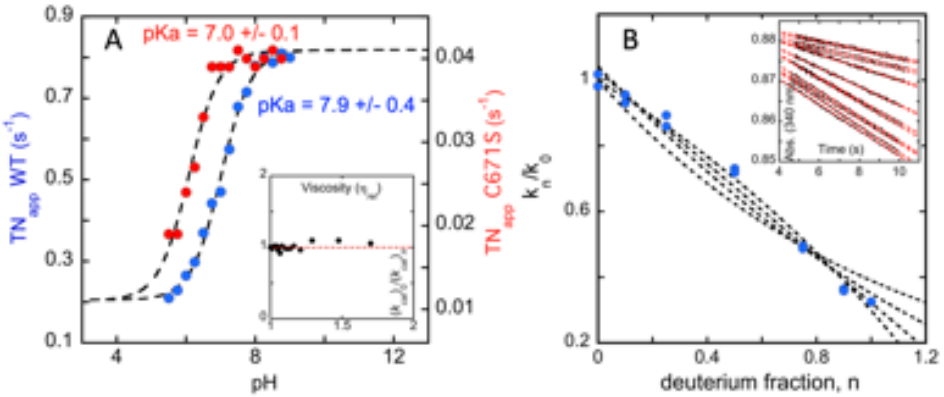

Figure 2. pH Dependence for DPD WT and C671S and steady-state solvent isotope effects or DPD WT. **A**. Determination of the macroscopic pKa for the apparent turnover number of DPD WT (blue) and DPD C671S (red). A solution containing 1 µM of enzyme prepared in dilute MAT buffer (1/100) was mixed with 150 µM NADPH and 150 µM uracil prepared in MAT buffer adjusted to the desired pH between 5.5 and 8.5. The apparent turnover (TN_{app}) number was determined by observing the reaction at 340 nm for 50 seconds and fitting the initial data from 2-20 seconds to a straight line. The pH-dependence of the TN value was fit to Equation 1. Inset depicts the viscosity effect control for the C671S variant as a proxy for both enzymes. For this control 2.5 µM DPD C671S in dilute MAT buffer (1/100) pH 7.5 was combined with 150 µM NADPH and 150 µM uracil in MAT buffer pH 8.5 with various fractions of glycerol and observed at 340 nm. Rates were determined from the linear portion of the trace (2 - 20 sec). **B**. Proton inventory for DPD WT. The number or protons in flight in the pyrimidine reduction transition state was assessed by reacting 1 µM DPD WT in dilute MAT buffer (1/100) pH 7.5 with 150 µM NADPH and 150 µM uracil in MAT buffer pH 8.5. Inset shows traces of reactions monitored at 340 nm for 50 sec at 20 °C in buffer containing the desired deuterium fraction. Rates were determined from the linear portion of the trace (5 - 10 sec). The data were fit to Equation 2 (most concave), Equation 3 (for the two- (concave) and one-proton (linear) cases) and Equation 4 (convex).

Our data indicate single pKas of 7.92 ± 0.41 and 7.02 ± 0.04 for WT DPD and the C671S variant respectively (Figure 2). While the pK_a value for the former could be ascribed to the native C671 residue, the latter cannot be correlated with a serine residue in this position. Moreover, similar to previous reports the TN increased to a limit with increasing pH, which is counter to the expectation if the protonation of the residue at 671 was a requirement for turnover. These data suggest that the titration of a group other than the thiol of C671 is influencing the rate of pyrimidine reduction. The pKa of free $FMNH_2$ is derived from titration of the N1 proton to give the neutral or anionic forms and has been shown to be 6.7; qualitatively similar to the pKa's observed [41].

The effect of the deuterium fraction of solvent on the observed TN was assessed and used to obtain a proton inventory for WT DPD. Reactions were carried out in MAT buffer for reasons discussed above. A pL of 8.5 was selected as it is a pL independent region of the activity curve (Figure 2A). As a control, the TN was also assessed over a range of glycerol concentrations to

account for viscosity changes with the introduction of D_2O (η_{rel},1.25). These data indicate no dependence of the observed rate of turnover on solvent viscosity, consistent with rate limiting chemistry (Figure 2A)[42]. The results of the reaction of DPD with saturating uracil and NADPH clearly show that the steady-state rate of turnover is influenced by the concentration of solvent deuterium. The proton inventory data sets were fit to one and two-protons in flight and solvent medium effect equations (Equations 2 and 3, respectively) that each assume fractionation factors of one. The data were also fit to Equation 4 that accounts for fractionation factors for the hydron donating species in the reactant and transition states as would be expected for the involvement of a thiol acid. The shape of the dependence was observed to be convex and best fit to Equation 4 that assumes the movement of a single proton that exhibits fractional deuterium substitution. The fits returned a solvent kinetic isotope effect (SKIE), defined here by φ^R/φ^T, of 3.35 ± 0.50. It is conceivable that the curve could also be described by the movement of two protons, however the data presented does not have the precision to effectively discriminate between these cases. Two exchangeable hydrogens are transmitted to the pyrimidine during reduction of the base; one proton from the active site acid C671, and one as a hydride from the reduced FMN N5 position. It is surmised that the transfer of these hydrogens is simultaneous and contingent on the availability of the C671 proton as the C671A variant is not catalytic and the C671S variant has a markedly slower rate of turnover[30]. Together the pH profile and the SKIE data suggest, that one or more hydrogens are displaced in the transition state for pyrimidine reduction and that one of these is likely derived from the C671 thiol and that the deprotonation of a group at or near the reduced FMN promotes the rate of pyrimidine reduction by fourfold.

***Transient-state pH effects on the reductive activation of the DPD C671S variant*:** As stated, the C671S variant of DPD exhibits pronounced delineation in terms of observed rate constants for the reductive activation and ensuing turnover events[30]. The effect of pH on the reductive activation reaction of the C671S variant with saturating thymine was assessed under single-turnover conditions with limiting NADPH. The traces obtained at 340 nm revealed further resolution of the activation phase at low pH values (Figure 3A) and were fit to a combination of 2 exponentials and a linear phase (Equation 4).

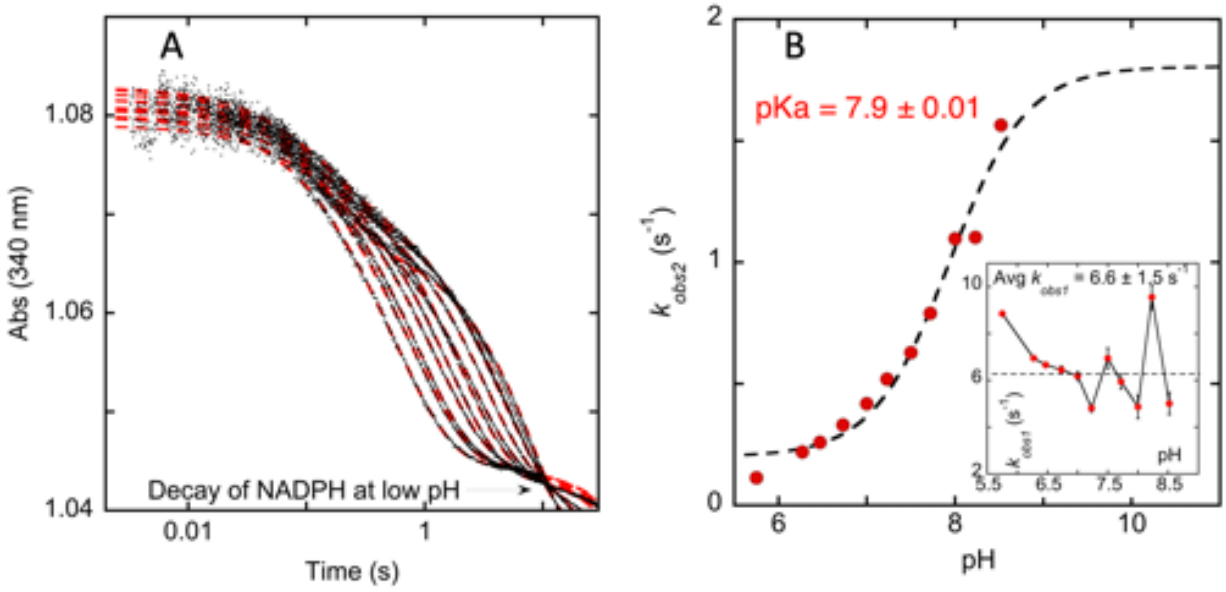

Figure 3. The effect of pH on the activation phase of C671S DPD. **A**. The effect of pH was assessed by mixing 10 µM of DPD C671S with 50 µM NADPH and 100 µM thymine at varying pH values (5.75, 6.0, 6.3, 6.5, 6.7, 7.0., 7.2, 7.5, 7.72, 8.0, 8.23, 8.52) under anaerobic conditions. The reaction was monitored at 340 nm for 10 seconds at 20 °C. **B**. The dependence of the rate for the second phase (k_{obs2}) on pH when the rate of k_{obs1} is fixed to the mean value of 6.6 s^{-1} that was determined from rates returned from fitting to a combination of exponentials (Equation 4). Data were fit to Equation 1.

The two initial exponential phases (k_{obs1} and k_{obs2}) report the steps of reductive activation that consumes two electrons from NADPH[30]. A linear phase was added to qualitatively account for denaturation of NADPH at low pHs. The value for k_{obs1} derived from the fit scattered for different pH values about a mean of 6.6 ± 1.5 s^{-1} but did not titrate predictably with pH. The value returned

for k_{obs2} (when k_{obs1} is fixed to its mean) was plotted against the pH of the reaction. The data in Figure 3B was fit to Equation 1 and returned a pK_a of 7.9 ± 0.01 where k_{obs2} had a positive dependence on the concentration of hydroxyl ions. Previous experiments at pH 7.5 were largely monophasic for activation as was observed in the data presented here. Lower pH values appear to slow the hydride transfer for activation and separate the data into two phases. The pH dependent phase in prior work was shown to report the oxidation of NADPH and the concomitant reduction of a flavin cofactor[30]. Our data suggest that these electrons cross the protein and reside on the FMN yielding the active form of DPD. The observed pKa of 7.9 for the activation step differs from the value observed for the pH dependence of turnover with this variant (pKa - 7.0, Figure 2A). As such we tentatively ascribe the pK_a observed as arising from a deprotonation within the region of hydride transfer at the FAD and suggest that the protonation state of this group(s) influences the rate of reductive activation. Prior to activation both flavins are oxidized and would exhibit pKa values at the extremes of the pH range and markedly distant from 7.9. It is therefore reasonable to conclude that the pKa observed is for groups proximal to one or both of the flavin cofactors that when protonated impede the propensity of the isoalloxazine(s) to receive electrons.

Spectrophotometric deconvolution of DPD reductive activation: The delineation of the activation process into two phases (Figure 3) provided an opportunity to identify and assign more of the chemistry involved. For both the C671S and C671A variants the activation process was observed by CCD spectrophotometric detection and the three-dimensional datasets obtained

were deconvoluted by singular value decomposition to give the pure spectra of the participating states (Figure 4).

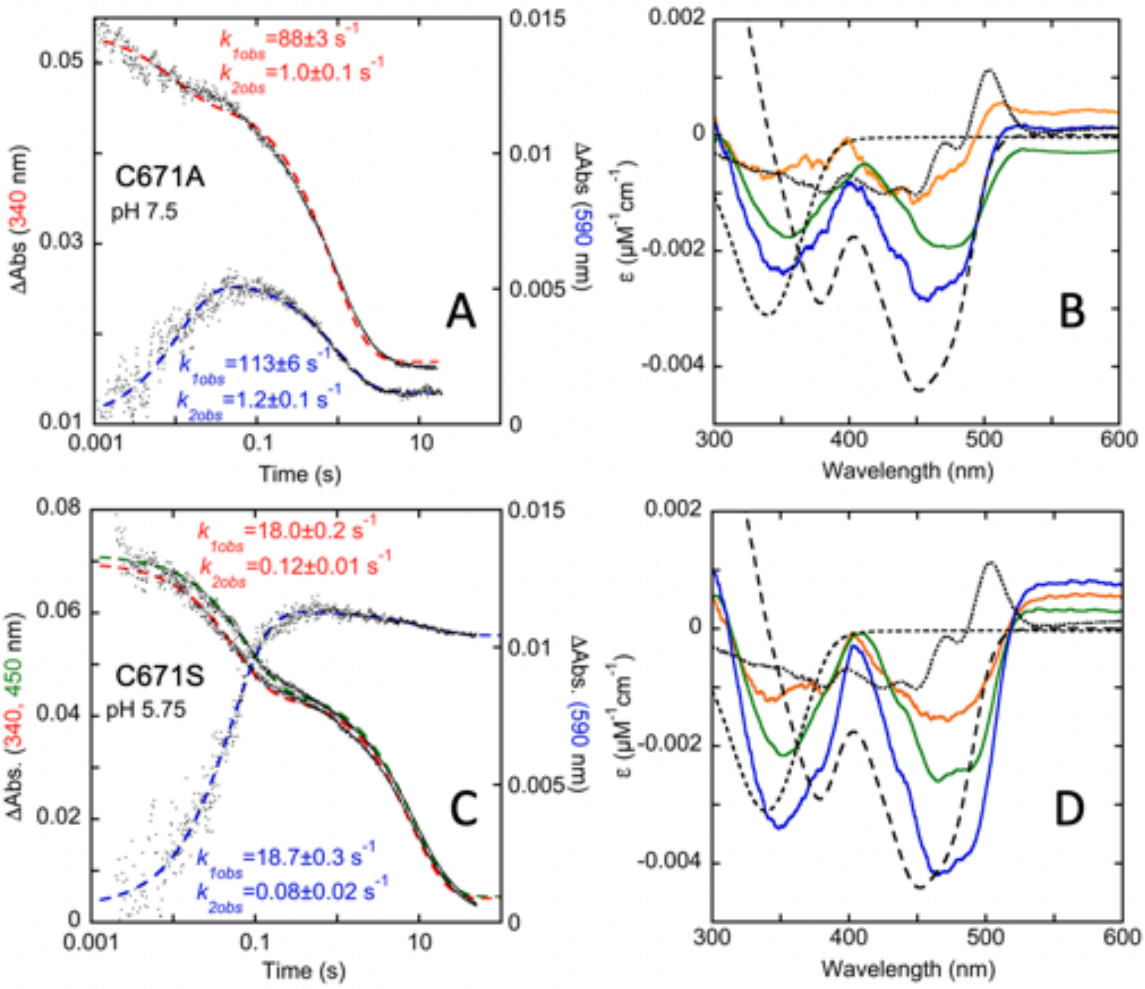

Figure 4. Deconvolution of DPD C671S and C671A Activation Events. **Top.** DPD C671A (15 μM) was mixed with NADPH (13 μM) in the presence of thymine (100 μM). **A.** Absorbance changes observed at 340 nm (red) and 580 nm (blue) for the reductive activation of DPD C671S. The data were fit to a linear combination of two exponentials according to Equation 5 which returned rate constants as shown. **B.** Difference spectra derived from component spectra derived from singular value decomposition of the absorption changes observed during activation of DPD C671A. Orange, difference spectrum for phase 1. Green, difference spectrum for phase 2, Blue net difference spectrum for both phases. Overlaid are reference difference spectra for reduction of a flavin/2 (large dashes), oxidation of NADPH/2 (small dashes), binding of $NADP^+$ at pH 7.5 (dotted). **Bottom.** DPD C671S (14 μM) was mixed with NADPH (50 μM) in the presence of thymine (100 μM). **C.** Absorbance changes observed at 340 nm (red), 450 nm (green) and 580 nm (blue) for the reductive activation of DPD C671S. The data were fit to a linear combination of two exponentials according to Equation 5 which returned rate constants as shown. **D.** Difference spectra derived from component spectra from singular value decomposition of the absorption changes observed during activation of DPD C671S. Orange, difference spectrum for phase 1. Green, difference spectrum for phase 2, Blue net difference spectrum for both phases. Overlaid are reference difference spectra for the reduction of a flavin/2 (large dashes), oxidation of NADPH/2 (small dashes), binding of $NADP^+$ at pH 5.75 (dotted).

Subtraction of successive spectra then yielded the net absorption changes in the intervening step. The NADPH concentrations used for each variant differed and so each dataset revealed unique aspects of the activation process.

DPD C671A variant eliminates the proton coupled electron transfer required to reduce pyrimidine substrates. However, the variant is observed to take up electrons from NADPH and activate in the presence of substrate pyrimidines. This variant exhibited delineation of the activation steps at pH 7.5 (Figure 4A). The data indicate that charge transfer absorption centered around 590 nm accumulates at ~100 s^{-1}, concomitant with the first phase of activation. This charge transfer then decays at ~1.1 s^{-1}. The decay corresponds to the net hydride transfer that reduces one of the two flavins of the protomer. Consistent with these conclusions, spectrophotometric deconvolution revealed that the first phase does not include oxidation of NADPH or reduction of a flavin (Figure 4B, orange spectrum). The difference spectrum for the species that accumulates in the first phase instead is qualitatively similar to difference spectrum for binding of $NADP^+$ (Figure 4B, dotted spectrum) added to the charge transfer feature centered around 580 nm. Together these data report the association of NADPH in the first phase observed[43]. In the methods used DPD C671A variant was combined with both NADPH and thymine simultaneously. That no evidence of the distinctive pyrimidine binding difference spectrum[30] was captured indicates that pyrimidine binding is rapid relative to NADPH association. The difference spectrum for the ensuing step indicates oxidation of NADPH added to the absorption changes for reduction of a flavin (Figure 4B, green spectrum) denoting that the second phase is the two-electron activation step. Aspects of these data deviate from expectation. It is unclear why the sum of the difference spectra for both phases does not equal to the absorption

changes expected for reduction of one flavin per dimer. Moreover, if only a fraction of the C671A sample is stimulated to activate as the net changes would indicate, it is not apparent why the charge transfer band would not persist in the presence of the residual unreacted NADPH. These inconsistencies suggest that the C671A variant sample was partially non-functional.

The C671S variant exhibits both delineation of reductive activation into two phases at low pH values and exceptionally slow turnover with thymine (0.00024 s^{-1}) [30]. This variant therefore can be induced to behave similarly to the C671A variant and ostensibly isolate the observation of reductive activation events from subsequent reduction of pyrimidine. In these experiments the concentration of NADPH was fourfold that of the variant (Figure 4C). The purpose of the excess reductant was to demonstrate where the electrons acquired during activation reside within the catalytically active enzyme. If the origin of charge transfer is NADPH•FAD complex, exchange of the $NADP^+$ formed during activation with exogenous NADPH will reinstate/maintain the charge transfer absorption indicating that reduced FAD does not accumulate in the reductive activation reaction. Accordingly, it was observed that excess NADPH promoted sustained charge transfer indicating that the FAD is oxidized in the activated state of the enzyme. The rate of accumulation of this absorption is again coincident with a decrease at all wavelengths between 300 and 500 nm that occurred with a rate constant of ~18 s^{-1} (Figure 4C). This absorption then diminished slightly as the enzyme was reduced with a rate constant of 0.08 s^{-1}. However, for this variant, the difference spectrum associated with the first phase does not have character indicative of NADPH binding and would appear to be dominated by partial flavin reduction that presumably occurred with excess NADPH. The subsequent reductive phase is tenfold slower than

observed with the C671A variant as was expected at pH 5.75, but in this case the net extinction coefficient changes are consistent with the reduction of ~one flavin per dimer.

Structural evidence for the activated state of DPD: Kinetic evidence presented herein and in prior studies indicate that the active form of DPD is two-electron reduced. The evidence obtained has implied that electrons from NADPH transiently reduce the FAD but rapidly traverse the protein and reside on the FMN cofactor. The prior evidence for this conclusion was principally that DPD dioxygen reactivity was suppressed by the addition of pyrimidine.[30] Herein, we have presented additional kinetic evidence that the electrons acquired in activation reside on the FMN cofactor. To obtain structural evidence for activation, crystals of DPD variants C671S and C671A were soaked in NADPH and pyrimidine substrates under low oxygen partial pressure in attempt to capture the activated form of the enzyme. As stated, the C671S variant has extraordinarily slow rate of turnover with thymine as a substrate; completing a single turnover in approximately 50,000 seconds[30]. This form of the enzyme therefore has an extended period after activation before significant turnover has occurred, during which the activated state of the enzyme could be captured in the crystal and structurally resolved. Similarly, the C671A variant is incapable of completing turnover with pyrimidine substrates but retains the reductive activation process. As such, crystals of both forms of the enzyme were soaked in NADPH and pyrimidine for 20 minutes (largely in the absence of dioxygen) and then frozen in liquid nitrogen.

The C671S variant structure was solved to 1.69 Å resolution and is the most complete structure of DPD yet reported, missing density only for residues 675-678 (MGER). The asymmetric unit includes two dimers (AB-CD) and the A subunit is representative of the four protomers.

Importantly, the relative high resolution of this structure permitted the discrimination of configurational differences for the flavin cofactors. These data are consistent with the proposed activated state of the enzyme that has the FMN cofactor reduced.

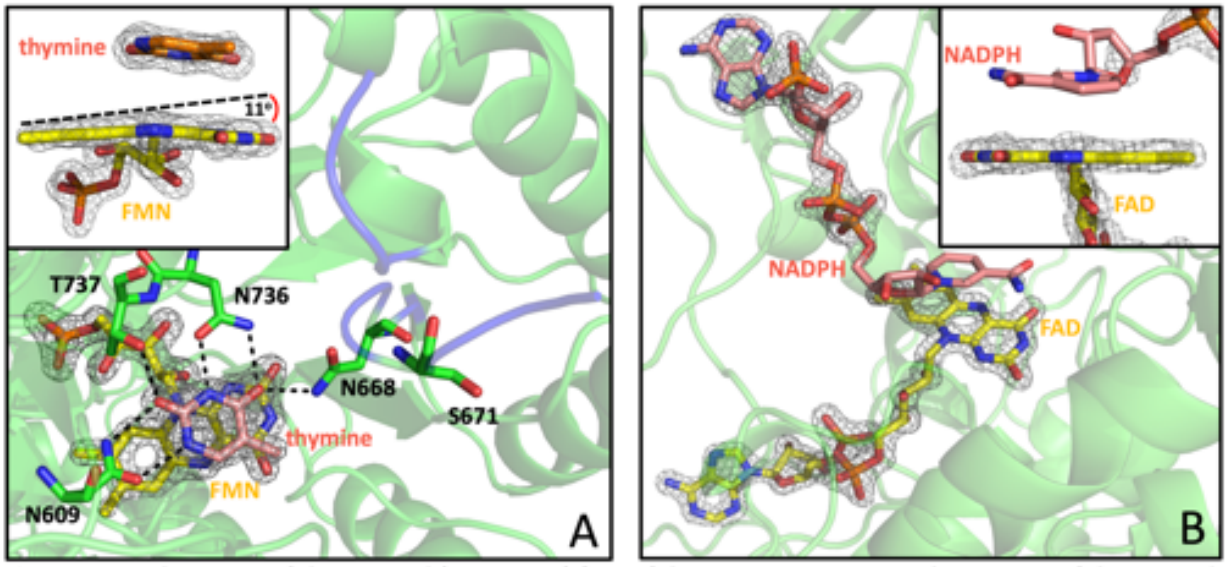

Figure 5. Crystal structure of the activated (DPD-FMNH·) form of the DPD C671S variant in the presence of thymine and NADPH (PDB ID: 7M31). Density is for the omit map was contoured at 2.0σ and was generated by excluding, FAD, FMN, NADPH, thymine and S671 for the model. **A.** Pyrimidine active site with bound thymine (pink) and FMN (yellow). All residues within hydrogen bonding distance of thymine are shown as green sticks and the mobile loop is shown in blue. **B.** NADPH binding site with bound NADP(H) (pink) and FAD (yellow). Insets, close-up of active site ligands. The angle (pucker) of the flavin isoalloxazine is indicative of the oxidation state of the flavin; pucker indicates a reduced flavin.

This cofactor while confined by the pyrimidine substrate and residues that stack closely on the *re* and *si*-faces of the isoalloxazine, exhibits an 11° pleat at the N1 and N5 axis, suggesting that the destination of the initial two electrons from NADPH that activate the enzyme (Figure 5A inset). In addition, the density for the FAD isoalloxazine ring is flat within angle error for this structure and was modeled in the oxidized state consistent with the predicted net oxidation state for the activated form of DPD (Figure 5B inset). Importantly, all prior published structures of DPD, some of which were solved to higher resolution, have density for the FMN that indicates the isoalloxazine is planar[21, 22, 44]. While the source of the electrons cannot be definitively known for method that utilizes ionizing radiation, it can reasonably be claimed that this is the first DPD

structure to exhibit a reduced cofactor. Regardless of the source of the electrons, this structure was solved in the presence of excess NADPH and is representative of the proposed state of the activated enzyme charge-transfer complex observed in Figure 4C & D.

In the C671S structure, the thymine substrate is positioned over the $FMNH_2$ cofactor with the 6-methyne carbon 3.3 Å from the flavin N5. The variant serine residue is 11.1 Å from the thymine 5-position that would ultimately receive the proton from this side chain. As such this structure captures a state of the enzyme that precedes reduction of the pyrimidine in which the active site general acid, located on the only mobile structural element within the protein, is distant from this substrate. Conformational mobility for residues 669-684 has been observed in multiple structures of DPD and the presumed function of this movement is to gate ingress and egress of pyrimidines and potentially shelter the reaction from solvent[21, 22]. That this loop was captured in a conformation that places the 671 general acid distant from the site of protonation suggests that catalytic turnover in the crystal lattice is impeded in addition to the pronounced slow turnover exhibited by this variant with thymine as a substrate[30].

The C671A variant structure that was generated from crystals soaked in a similar manner to those of C671S did not reveal definitive evidence of the reduction state of either flavin cofactor. The reason for this was presumably the slightly lower resolution obtained for this structure (1.82 Å). This structure is presented only to illustrate the contrast for what was ascertained at each level of resolution (Figure S1). Nonetheless, $FMNH_2$ was the cofactor oxidation state that best fit the density observed.

Transient-state kinetic isotope effects: Transient-state kinetic isotope effects (KIE) were assessed by observing the successive activation and turnover phases of DPD C671S at 340 nm in the presence of either NADPH or Pro-S NADPD[22]. For both substrates $NADP^+$ was enzymatically reduced using the same methods to avoid observing changes in rates derived from contaminants specific to the preparatory protocol. When observed at 340 nm, the Pro-S NADPD substrate resulted in a kinetic isotope effect of 1.90 ± 0.03 on the activation phase of DPD and the ensuing turnover phase was unaffected by the nicotinamide-derived deuterium (Figure 6).

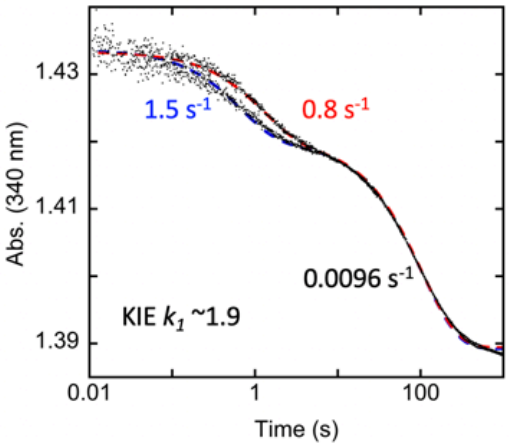

Figure 6. Transient state kinetic isotope effects. C671S variant (15 µM) in MAT buffer prepared anaerobically mixed with saturating uracil (100 µM) and either NADPH (blue) or NADPD (red) (both 9 µM). Traces were collected under single turnover conditions monitored and at 340 nm for 1000 seconds at 20 °C. Data was fit to a combination of exponentials (Equation 5).

This indicates that hydride transfer from NADPH to the FAD isoalloxazine is rate limiting in activation. Assuming that the oxidation of $FADH_2$ is rapid, the deuteride that is transferred to the FAD N5 slows the observed rate of reduction of the FMN. In this manner the FMN is acting as an electron sink, drawing electrons across the assumed barrier-less/low resistance of the FAD, iron-sulfur center conduit. Reductive activation in this manner requires protonation of the FMN N5

via an active site general acid. The only residue observed to be proximal to this position is Lysine 574 (3.1 Å) which has a conformation that places the amine in line with the plane of the isoalloxazine, an appropriate position to both protonate the sp^2-hybridized N5 of the oxidized form of this cofactor.

Discussion

The fundamental curiosity of DPD is the complexity of the enzyme relative to the chemistry catalyzed (Figure 1, Scheme 1). Flavoproteins that catalyze dehydrogenation reactions typically have ping-pong mechanisms that have an intervening reduced state of the flavin that exchanges oxidized substrates. These enzymes can be studied comprehensively using transient-state methods as reductive and oxidative half-reactions by omitting substrates required for the preceding or ensuing half-reaction. Our recent publications have shown that DPD cannot be studied using transient-state half-reactions. The reason for this is that once the enzyme has undergone reductive activation no further reduced form of any of the cofactors is observed during catalysis. The overarching conclusion is that the internal electron transfer rate is rapid relative to the low rate of turnover (WT DPD 0.9 s^{-1}) which is defined by a slow process on which electron transfer is contingent.

We recently published two transient-state and structural investigations of DPD that revealed the active state of DPD is two-electron reduced and that these electrons come from NADPH and reside on one of the two flavins within the enzyme[30, 40]. In this study we consolidate these observations with further investigation of the observable steps of reductive activation and turnover reactions. Reductive activation of the enzyme is an initial process prior to catalytic turnover that is observed as a consequence of the enzyme being isolated under aerobic conditions ensuring that all cofactors are oxidized. In single turnover reactions of the WT enzyme, the reductive activation step is not kinetically distinct from the subsequent turnover phase. As such, in most instances we have employed the C671S variant of DPD that alters the pyrimidine active site general acid and slows the rate of catalytic turnover to a greater extent than the rate

of reductive activation. This kinetic delineation of functionally separate processes has permitted a more focused investigation of what occurs in each[30].

The pH-dependence of the apparent rate of turnover indicated that deprotonation of a group or groups with a net pKa of ~8 increases the rate of catalysis by fourfold (Figure 2A). This is opposite for what is expected for the titration of an active site acid residue. Moreover, this pKa is changed to 7 in the C671S variant indicating that the rate is not defined by the pKa of the residue in the 671 position. We tentatively conclude that the pKa reports the protonation state of the adjacent $FMNH_2$ cofactor that has more capacity to delocalize electrons when the N1-position is deprotonated and thus is more competent to reduce the pyrimidine. However, we do not attribute the protonation state of the FMN as defining the rate of turnover, but rather that the anionic form of this cofactor increases the probability that pyrimidine reduction will occur (see below).

The convex shape of the proton inventory data for the rate of pyrimidine reduction reveal that DPD has a hydrogen in flight in the transition state for the step that reduces the pyrimidine substrate that has fractional deuterium occupancy in D_2O solvent (Figure 2B). These data, however, do not definitively distinguish between one and two hydrogens in flight and so do not unambiguously resolve the mechanism of pyrimidine reduction. The data are however consistent with the donation of the C671 proton in the rate limiting step. The hydrogen bonded to the N5 position of $FMNH^-$ is also subject to exchange with solvent and the transfer of this hydride must occur in the same step unless the transient formation of a pyrimidine anion is proposed. However, Tthe formation of such a species can be discounted by the fact that the C671A variant is incapable of pyrimidine reduction.

The N5 hydrogens of both $FADH_2$ and $FMNH^-$ are displaced during turnover; however, the hydride that was donated to the FAD N5 from NADPH is displaced as a hydrogen when in D_2O solvent only if the rate of electron transmittance from this cofactor greatly exceeds the rate of solvent exchange. That the rate of turnover is unaffected when Pro-S NADPD is used as a substrate (Figure 6) indicates that the required displacement of the N5-deuterium from the reduced FAD is rapid, validating the proposal that electrons are, in both activation and turnover, rapidly transmitted forward from $FADH_2$. That activation of the C671S variant can be further resolved into two phases at low pH, that binding of NADPH is the first process observed and that reduction of the FMN is the second (Figure 4A & B), indicates that the rate of activation is limited by the rate of hydride transfer from NADPH to FAD and not the rate of oxidation of $FADH_2$ (Figure 3A). This conclusion is supported by the fact that the pKa of ~8 observed for the limiting rate of activation differs from the pKa observed for the turnover phase for this variant (Figure 2, pKa of 7), suggesting that the pKas arise from the titration of separate groups. These are tentatively ascribed to a deprotonation event near the FAD that increases the rate of hydride transfer from NADPH in reductive activation and deprotonation of another group at or near the reduced FMN that increases the rate of pyrimidine reduction in turnover.

Evidence that transmittance of electrons across the protein is facile and rapid relative to the rate of turnover is based in the observation that the absorption of the enzyme's cofactors is largely unchanging in turnover[30]. Other than small perturbations of both flavin spectra in response to substrate/product association, no further reduced state of the enzyme is observed. This is interpreted as the substrate and cofactor set utilizing a Newton's cradle mechanism in which two-electrons enter the system from NADPH as two electrons are displaced onto the

pyrimidine, without the accumulation of an intervening reduced state for any cofactor[30]. This is not a perfect analogy as exchange of electrons between adjacent cofactors in the conduit would occur in a single-electron and stepwise manner, but the speed of these exchanges means that observationally electrons enter the system with the same rate at which they exit. The requirement for single electron steps is supported by the data of Lohkamp et al., who established that non-activated DPD is EPR silent indicating that the Fe_4S_4 centers are in the 2+ state and populated only with Fe(II) ions[45], in this state the clusters can conventionally only accept one electron. Moreover, stoichiometry measurements for NADPH consumption and the structural data presented here indicate that these centers do not change oxidation state with reductive activation[30]. One illustrative implication of this for the activated form of the enzyme is that the two electrons provided by NADPH are used only to reinstate the oxidation state of the $FMNH_2$ cofactor and thus reduce the pyrimidine substrate that is acquired with the subsequent turnover. Further evidence for rapid electron transfer is found in the activation step that establishes the functional oxidation state of the FMN (Figure 4). The accumulation of NADPH•FAD charge transfer is observed without observation of reduced FAD, indicating that electrons from NADPH rapidly traverse the protein.

Figure 7 summarizes the observed and inferred processes of the C671S DPD activation and turnover reactions. While not comprehensive for all possible random binding and release steps, the scheme does illustrate a mechanism consistent with the observations made here and in our prior publications[30, 44]. This scheme indicates that the observed rate of turnover of DPD is slow despite proposed rapid electron transmittance[30]. As such, we must conclude that some other factor limits the rate of turnover.

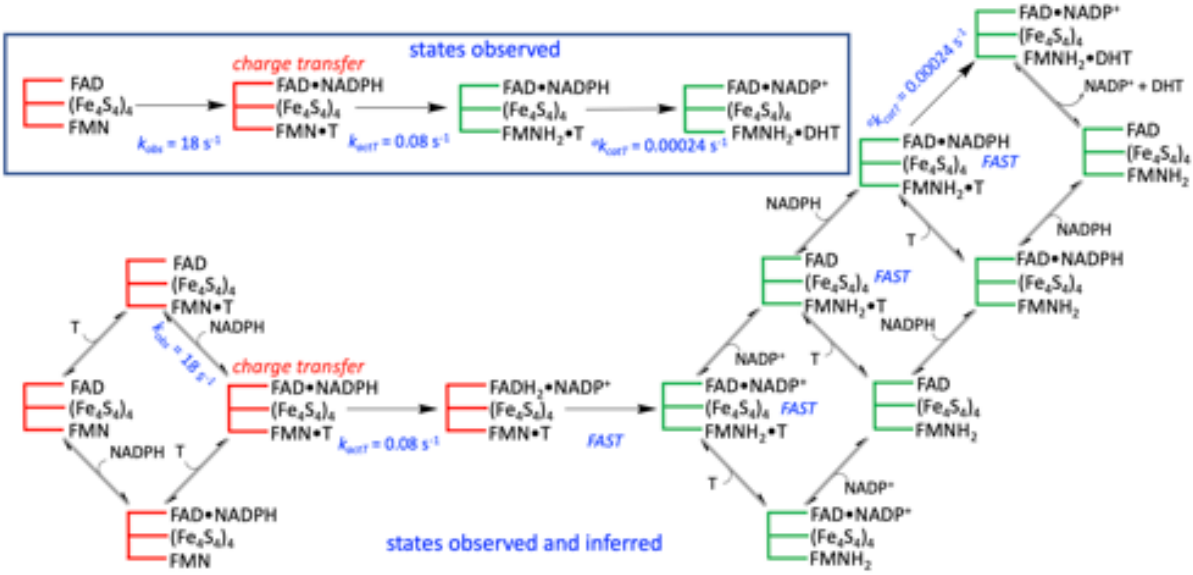

Figure 7. Observed and Inferred steps in DPD C671S Activation and Turnover with Thymine. Non-activated enzyme is shown with a red cofactor scaffold and active with a green scaffold. The primary scheme depicts all steps observed and inferred while the boxed reaction sequence depicts only what is observable. *a* – taken from Beaupre et al., 2020 Biochemistry, 59 pp 2419-2431.

We propose that for the activated enzyme the input of electrons from NADPH at the FAD site is controlled by the positioning of the distant 671 residue (C or S) that when proximal to the pyrimidine substrate completes the proton-coupled electron-transfer conduit. We and others have observed that the loop bearing the 671 residue is the only structural feature to exhibit multiple conformations in X-ray crystal structures[22, 48]; and this loop is observed to be dynamic even when the C671 residue is covalently tethered to a reactive substrate analog [21, 22, 44]. While the donation of the proton supplied by this residue is assumed to be facile, the relative scarcity of the proton arising from movement of the 669-684 loop is suggested to be the primary governing factor in the rate of catalysis.

Supporting Information

Contents:

References

[1] Lu, Z. H., Zhang, R., and Diasio, R. B. (1992) Purification and characterization of dihydropyrimidine dehydrogenase from human liver, *J Biol Chem 267*, 17102-17109.

[2] Podschun, B., Jahnke, K., Schnackerz, K. D., and Cook, P. F. (1993) Acid base catalytic mechanism of the dihydropyrimidine dehydrogenase from pH studies, *J Biol Chem 268*, 3407-3413.

[3] Podschun, B., Cook, P. F., and Schnackerz, K. D. (1990) Kinetic mechanism of dihydropyrimidine dehydrogenase from pig liver, *J Biol Chem 265*, 12966-12972.

[4] Longley, D. B., Harkin, D. P., and Johnston, P. G. (2003) 5-fluorouracil: mechanisms of action and clinical strategies, *Nat Rev Cancer 3*, 330-338.

[5] de Bono, J. S., and Twelves, C. J. (2001) The oral fluorinated pyrimidines, *Invest New Drugs 19*, 41-59.

[6] Heidelberger, C. (1963) Biochemical Mechanisms of Action of Fluorinated Pyrimidines, *Exp Cell Res 24*, SUPPL9:462-471.

[7] Kent, R. J., and Heidelberger, C. (1972) Fluorinated pyrimidines. XL. The reduction of 5-fluorouridine 5'-diphosphate by ribonucleotide reductase, *Mol Pharmacol 8*, 465-475.

[8] Milano, G., and Etienne, M. C. (1994) Dihydropyrimidine dehydrogenase (DPD) and clinical pharmacology of 5-fluorouracil (review), *Anticancer Res 14*, 2295-2297.

[9] Heggie, G. D., Sommadossi, J. P., Cross, D. S., Huster, W. J., and Diasio, R. B. (1987) Clinical pharmacokinetics of 5-fluorouracil and its metabolites in plasma, urine, and bile, *Cancer Res 47*, 2203-2206.

[10] Reilly, R. T., Barbour, K. W., Dunlap, R. B., and Berger, F. G. (1995) Biphasic binding of 5-fluoro-2'-deoxyuridylate to human thymidylate synthase, *Mol Pharmacol 48*, 72-79.

[11] Ludwiczak, J., Maj, P., Wilk, P., Fraczyk, T., Ruman, T., Kierdaszuk, B., Jarmula, A., and Rode, W. (2016) Phosphorylation of thymidylate synthase affects slow-binding inhibition by 5-fluoro-dUMP and N(4)-hydroxy-dCMP, *Mol Biosyst 12*, 1333-1341.

[12] Moloney, M., Faulkner, D., Link, E., Rischin, D., Solomon, B., Lim, A. M., Zalcberg, J. R., Jefford, M., and Michael, M. (2018) Feasibility of 5-fluorouracil pharmacokinetic monitoring using the My-5FU PCM system in a quaternary oncology centre, *Cancer Chemother Pharmacol 82*, 865-876.

[13] Porter, D. J., Chestnut, W. G., Merrill, B. M., and Spector, T. (1992) Mechanism-based inactivation of dihydropyrimidine dehydrogenase by 5-ethynyluracil, *J Biol Chem 267*, 5236-5242.

[14] Baccanari, D. P., Davis, S. T., Knick, V. C., and Spector, T. (1993) 5-Ethynyluracil (776C85): a potent modulator of the pharmacokinetics and antitumor efficacy of 5-fluorouracil, *Proc Natl Acad Sci U S A 90*, 11064-11068.

[15] Spector, T., Harrington, J. A., and Porter, D. J. (1993) 5-Ethynyluracil (776C85): inactivation of dihydropyrimidine dehydrogenase in vivo, *Biochem Pharmacol 46*, 2243-2248.

[16] Porter, D. J., Harrington, J. A., Almond, M. R., Lowen, G. T., Zimmerman, T. P., and Spector, T. (1994) 5-ethynyl-2(1H)-pyrimidinone: aldehyde oxidase-activation to 5-ethynyluracil, a mechanism-based inactivator of dihydropyrimidine dehydrogenase, *Biochem Pharmacol 47*, 1165-1171.

[17] Dulchavsky, M., Clark, C. T., Bardwell, J. C. A., and Stull, F. (2021) A cytochrome c is the natural electron acceptor for nicotine oxidoreductase, *Nature chemical biology 17*, 344-350.

[18] Fagan, R. L., Nelson, M. N., Pagano, P. M., and Palfey, B. A. (2006) Mechanism of flavin reduction in class 2 dihydroorotate dehydrogenases, *Biochemistry 45*, 14926-14932.

[19] Fagan, R. L., Jensen, K. F., Bjornberg, O., and Palfey, B. A. (2007) Mechanism of flavin reduction in the class 1A dihydroorotate dehydrogenase from Lactococcus lactis, *Biochemistry 46*, 4028-4036.

[20] Abramovitz, A. S., and Massey, V. (1976) Interaction of phenols with old yellow enzyme physical evidence for charge-transfer complexes, *J.Biol.Chem. 251*, 5327-5336.

[21] Dobritzsch, D., Ricagno, S., Schneider, G., Schnackerz, K. D., and Lindqvist, Y. (2002) Crystal structure of the productive ternary complex of dihydropyrimidine dehydrogenase with NADPH and 5-iodouracil. Implications for mechanism of inhibition and electron transfer, *J Biol Chem 277*, 13155-13166.

[22] Dobritzsch, D., Schneider, G., Schnackerz, K. D., and Lindqvist, Y. (2001) Crystal structure of dihydropyrimidine dehydrogenase, a major determinant of the pharmacokinetics of the anti-cancer drug 5-fluorouracil, *EMBO J 20*, 650-660.

[23] Podschun, B., Wahler, G., and Schnackerz, K. D. (1989) Purification and characterization of dihydropyrimidine dehydrogenase from pig liver, *Eur J Biochem 185*, 219-224.

[24] Schmitt, U., Jahnke, K., Rosenbaum, K., Cook, P. F., and Schnackerz, K. D. (1996) Purification and characterization of dihydropyrimidine dehydrogenase from Alcaligenes eutrophus, *Arch Biochem Biophys 332*, 175-182.

[25] Porter, D. J., and Spector, T. (1993) Dihydropyrimidine dehydrogenase. Kinetic mechanism for reduction of uracil by NADPH, *J Biol Chem 268*, 19321-19327.

[26] Rosenbaum, K., Schaffrath, B., Hagen, W. R., Jahnke, K., Gonzalez, F. J., Cook, P. F., and Schnackerz, K. D. (1997) Purification, characterization, and kinetics of porcine recombinant dihydropyrimidine dehydrogenase, *Protein Expr Purif 10*, 185-191.

[27] Rosenbaum, K., Jahnke, K., Curti, B., Hagen, W. R., Schnackerz, K. D., and Vanoni, M. A. (1998) Porcine recombinant dihydropyrimidine dehydrogenase: comparison of the spectroscopic and catalytic properties of the wild-type and C671A mutant enzymes, *Biochemistry 37*, 17598-17609.

[28] Shiotani, T., and Weber, G. (1981) Purification and properties of dihydrothymine dehydrogenase from rat liver, *J Biol Chem 256*, 219-224.

[29] Beaupre, B. A., Roman, J. V., and Moran, G. R. (2020) An improved method for the expression and purification of porcine dihydropyrimidine dehydrogenase, *Protein Expr Purif 171*, 105610.

[30] Beaupre, B. A., Forouzesh, D. C., and Moran, G. R. (2020) Transient-State Analysis of Porcine Dihydropyrimidine Dehydrogenase Reveals Reductive Activation by NADPH, *Biochemistry 59*, 2419-2431.

[31] Ellis, K. J., and Morrison, J. F. (1982) Buffers of constant ionic strength for studying pH-dependent processes, *Methods Enzymol 87*, 405-426.

[32] Rubinson, K. (2017) Practical corrections for p(H,D) measurements in mixed H2O/D2O biological buffers, *Anal. Methods 9*, 2744-2750.

[33] Moran, G. R. (2019) Anaerobic methods for the transient-state study of flavoproteins: The use of specialized glassware to define the concentration of dioxygen, *Methods Enzymol 620*, 27-49.

[34] Cleland, W. W. (1982) The use of pH studies to determine chemical mechanisms of enzyme-catalyzed reactions, *Methods Enzymol 87*, 390-405.

[35] Volk, A., and Kahler, C. J. (2018) Density model for aqueous glycerol solutions, *Exp Fluids 59*, Article 75.

[36] Venkatasubban, K. S., and Schowen, R. L. (1984) The proton inventory technique. 1. Introduction to proton inventories, *CRC Critical Rev.in Biochem. 17*, 1-44.

[37] Kohen, A., and Limbach, H. (2006) *Isotope Effects in Chemistry and Biology*, Vol. 1096, CRC Press.

[38] Kresge, A. (1964) Solvent isotope effect in H2O-D2O mixtures, *Pure and Appl. Chemistry 8*, 15.

[39] Holzerm, W., Shirdel, J., Zirak, P., Penzkoferm, A., Hegemann, P., Deutzmann, R., and Hochmuth, E. (2005) Photo-induced degradation of some flavins in aqueous solution, *Chemical Physics 308*, 69-78.

[40] Forouzesh, D. C., Beaupre, B. A., Butrin, A., Wawrzak, Z., Liu, D., and Moran, G. R. (2021) The Interaction of Porcine Dihydropyrimidine Dehydrogenase with the Chemotherapy Sensitizer: 5-Ethynyluracil, *Biochemistry 60*, 1120-1132.

[41] Yalloway, G. N., Mayhew, S. G., Malthouse, J. P., Gallagher, M. E., and Curley, G. P. (1999) pH-dependent spectroscopic changes associated with the hydroquinone of FMN in flavodoxins, *Biochemistry 38*, 3753-3762.

[42] Gadda, G., and Sobrado, P. (2018) Kinetic Solvent Viscosity Effects as Probes for Studying the Mechanisms of Enzyme Action, *Biochemistry 57*, 3445-3453.

[43] Massey, V., and Ghisla, S. (1974) Role of charge transfer interactions in flavoprotein catalysis, *Annals of the New York Academy of Sciences 227*, 446-465.

[44] Forouzesh, D. C., Beaupre, B. A., Butrin, A., Wawrzak, Z., Liu, D., and Moran, G. R. (2021) The Interaction of Porcine Dihydropyrimidine Dehydrogenase with the Chemotherapy Sensitizer: 5-Ethynyluracil, *Biochemistry*.

[45] Lohkamp, B., Voevodskaya, N., Lindqvist, Y., and Dobritzsch, D. (2010) Insights into the mechanism of dihydropyrimidine dehydrogenase from site-directed mutagenesis targeting the active site loop and redox cofactor coordination, *Biochim Biophys Acta 1804*, 2198-2206.

Acknowledgements

This research was supported by Loyola University College of Arts and Sciences and National Science Foundation Grant 1904480 to G.R.M.

Uniprot Identifiers

Sus Scrofa DPD - Q28943

For Table of Contents use only